THE JOURNAL OF BIOLOGICAL CHEMISTRY VOL. 290, NO. 10, pp. 6495–6506, March 6, 2015
Published in the U.S.A.

The Extracellular A-loop of Dual Oxidases Affects the Specificity of Reactive Oxygen Species Release*

Received for publication, July 8, 2014, and in revised form, January 11, 2015 Published, JBC Papers in Press, January 13, 2015, DOI 10.1074/jbc.M114.592717

Takehiko Ueyama[‡1], Megumi Sakuma[‡], Yuzuru Ninoyu[‡], Takeshi Hamada[‡], Corinne Dupuy[§], Miklós Geiszt[¶‖], Thomas L. Leto[**], and Naoaki Saito[‡2]

From the [‡]Laboratory of Molecular Pharmacology, Biosignal Research Center, Kobe University, Kobe 657-8501, Japan, [§]CNRS UMR8200 Laboratoire Stabilité Génétique et Oncogenèse, Université Paris-Sud, Institut Gustave Roussy, Villejuif 94805, France, [¶]Department of Physiology, Faculty of Medicine, Semmelweis University, H-1444 Budapest, Hungary, [‖]"Lendület" Peroxidase Enzyme Research Group of the Semmelweis University and the Hungarian Academy of Sciences, H-1444 Budapest, Hungary, and [**]Molecular Defenses Section, Laboratory of Host Defenses, NIAID, National Institutes of Health, Rockville, Maryland 20852

Background: Dual oxidase (Duox)-Duox activator (DuoxA) complexes produce H_2O_2, not $O_2^{\cdot-}$, suggesting that specialized mechanisms convert $O_2^{\cdot-}$ to H_2O_2.
Results: In comparison with Duox2, Duox1 prevents $O_2^{\cdot-}$ leakage more stringently.
Conclusion: Duox A-loops function in reducing $O_2^{\cdot-}$ release by promoting the stabilization and maturation of Duox-DuoxA complexes.
Significance: The mechanism underlying H_2O_2 production by Duoxes has been clarified.

NADPH oxidase (Nox) family proteins produce superoxide ($O_2^{\cdot-}$) directly by transferring an electron to molecular oxygen. Dual oxidases (Duoxes) also produce an $O_2^{\cdot-}$ intermediate, although the final species secreted by mature Duoxes is H_2O_2, suggesting that intramolecular $O_2^{\cdot-}$ dismutation or other mechanisms contribute to H_2O_2 release. We explored the structural determinants affecting reactive oxygen species formation by Duox enzymes. Duox2 showed $O_2^{\cdot-}$ leakage when mismatched with Duox activator 1 (DuoxA1). Duox2 released $O_2^{\cdot-}$ even in correctly matched combinations, including Duox2 + DuoxA2 and Duox2 + N-terminally tagged DuoxA2 regardless of the type or number of tags. Conversely, Duox1 did not release $O_2^{\cdot-}$ in any combination. Chimeric Duox2 possessing the A-loop of Duox1 showed no $O_2^{\cdot-}$ leakage; chimeric Duox1 possessing the A-loop of Duox2 released $O_2^{\cdot-}$. Moreover, Duox2 proteins possessing the A-loops of Nox1 or Nox5 co-expressed with DuoxA2 showed enhanced $O_2^{\cdot-}$ release, and Duox1 proteins possessing the A-loops of Nox1 or Nox5 co-expressed with DuoxA1 acquired $O_2^{\cdot-}$ leakage. Although we identified Duox1 A-loop residues (His^{1071}, His^{1072}, and Gly^{1074}) important for reducing $O_2^{\cdot-}$ release, mutations of these residues to those of Duox2 failed to convert Duox1 to an $O_2^{\cdot-}$-releasing enzyme. Using immunoprecipitation and endoglycosidase H sensitivity assays, we found that the A-loop of Duoxes binds to DuoxA N termini, creating more stable, mature Duox-DuoxA complexes. In conclusion, the A-loops of both Duoxes support H_2O_2 production through interaction with corresponding activators, but complex formation between the Duox1 A-loop and DuoxA1 results in tighter control of H_2O_2 release by the enzyme complex.

Dual oxidases (Duoxes[3]; Duox1 and Duox2) are members of the NADPH oxidase (Nox) family proteins (Nox1–5 and Duoxes) that produce reactive oxygen species (ROS) (1–3). Duox1 (4) and Duox2 (5) are functional only in combination with maturation factors known as Duox activators (DuoxAs; DuoxA1 and DuoxA2) (6). Although DuoxAs were first described as factors required to permit Duoxes to exit the endoplasmic reticulum, it was later reported that Duox and DuoxA proteins form stable heterodimers and co-translocate to the plasma membrane (7). Both Duoxes were first characterized as thyroid oxidases supporting thyroid hormone biosynthesis, although Duox2 is the dominant form, with an expression level five times higher than that of Duox1 in thyroid tissue (8). Moreover, mutations or deficiencies in Duox2 or DuoxA2 have been reported to cause congenital hypothyroidism in mice (9, 10) and humans (8), whereas deficiency in Duox1 has no effect on thyroid hormone levels in *Duox1* knock-out mice (11). Bi-allelic mutations in Duox2 reportedly cause transient congenital hypothyroidism, suggesting that some compensation occurs by Duox1 (12). More recently, a patient with transient congenital hypothyroidism was described; this patient was compound heterozygous for a large deletion comprising *DUOX2*, *DUOXA2*, and *DUOXA1* and a nonfunctional missense muta-

* This work was supported, in whole or in part, by the Intramural Research Program of the NIAID, National Institutes of Health. This work was also supported in part by a grant-in-aid for Scientific Research (C) of the Ministry of Education, Culture, Sports, Science and Technology, Japan, by a grant "Japan-Hungary Research Cooperative Program" from the Japan Society for the Promotion of Science and the Hungarian Academy of Sciences, by the Uehara Memorial Foundation, and by the Hyogo Science and Technology Association.

[1] To whom correspondence may be addressed: Laboratory of Molecular Pharmacology, Biosignal Research Center, Kobe University, 1-1 Rokkodai-cho, Nada-ku, Kobe 657-8501, Japan. Tel.: 81-78-803-5962; Fax: 81-78-803-5971; E-mail: tueyama@kobe-u.ac.jp.

[2] To whom correspondence may be addressed: Laboratory of Molecular Pharmacology, Biosignal Research Center, Kobe University, 1-1 Rokkodai-cho, Nada-ku, Kobe 657-8501, Japan. Tel.: 81-78-803-5962; Fax: 81-78-803-5971; E-mail: naosaito@kobe-u.ac.jp.

[3] The abbreviations used are: Duox, Dual oxidase; Nox, NADPH oxidase; DuoxA, Duox activator; $O_2^{\cdot-}$, superoxide; ROS, reactive oxygen species; PoxH, peroxidase homology; Endo H, endoglycosidase H; TM, transmembrane; pAb, polyclonal antibody; HBSS, Hank's balanced Salt Solution; aa, amino acids.

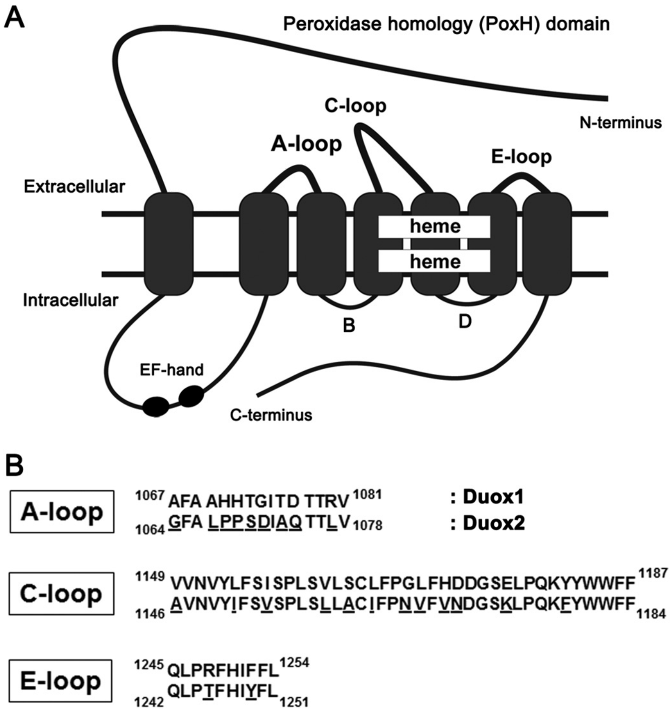

FIGURE 1. **Sequence alignment of the three extracellular loops of Duox1 and Duox2.** Schematic illustration of a Duox (*A*) and amino acid sequence alignment of the three extracellular loops (A, C, and E) of Duox1 and Duox2 (*B*) (4, 23). *Superscript* and *subscript numbers* represent amino acid sequence numbers. *Underlined residues* denote differences between Duox1 and Duox2.

tion of *DUOXA2* in the other allele, suggesting compensation by the remaining Duox1-DuoxA1 complex or by the mismatched Duox2-DuoxA1 complex (13).

In addition, Duox enzymes have been detected and believed to function on the epithelial cell surfaces of mucosal and exocrine tissues (2, 14–16), including the airways and gastrointestinal tract. In these tissues, Duoxes also function in host defense against a broad spectrum of pathogens (17–19). Nox family proteins produce the primary product superoxide ($O_2^{\cdot-}$) by directly transferring an electron to molecular oxygen (2, 20). Duoxes produce $O_2^{\cdot-}$ as an intermediate product (21), but the final product generated by mature Duoxes is H_2O_2, suggesting that intramolecular $O_2^{\cdot-}$ dismutation or other mechanisms contribute to H_2O_2 release (2). In tissues with high Duox expression, the enzymes accumulate on the apical plasma membrane, facilitating H_2O_2 release from epithelial cell surfaces to support the activities of extracellular hemoperoxidases (22).

In contrast to Nox1–5, Duoxes have an extended N-terminal extracellular domain called the peroxidase homology (PoxH) domain, followed by an additional transmembrane (TM) segment and an intracellular loop containing two calcium-binding EF-hand motifs (4, 23) (Fig. 1*A*). Thus, Duoxes possess four extracellular regions: the PoxH domain (1–595 amino acids (aa) in human Duox2) and three loops (the A-loop, 1064–1078 aa; C-loop, 1146–1184 aa; E-loop, 1242–1251 aa in human Duox2) (Fig. 1*A*). The PoxH domain is a candidate for intramolecular $O_2^{\cdot-}$ dismutation, although the isolated PoxH domains of both Duoxes demonstrate no $O_2^{\cdot-}$ dismutation activity *in vitro* (24, 25). Thus, the mechanism underlying H_2O_2 production by Duoxes remains poorly understood.

A switch in ROS generation from H_2O_2 to $O_2^{\cdot-}$ occurs when Duox2 is mismatched with DuoxA1 (26). We reported that the mismatched combination of Duox2 + DuoxA1, but not that of Duox1 + DuoxA2, releases $O_2^{\cdot-}$ in addition to H_2O_2; we called this phenomenon $O_2^{\cdot-}$ leakage (7). In this study we examined why Duox2, but not Duox1, leaks $O_2^{\cdot-}$, in addition to exploring the structural features of Duox and DuoxA proteins involved in H_2O_2 release. We found that the A-loops of Duoxes, particularly Duox1, function in controlling $O_2^{\cdot-}$ release by contributing to the stabilization and maturation of Duox-DuoxA complexes.

EXPERIMENTAL PROCEDURES

Materials—A polyclonal antibody (pAb) against Duoxes, which preferentially detects Duox2 via the first intracellular loop (639–1039 aa of human Duox2) but also detects Duox1, was previously described (15). A pAb against DuoxA1, which recognizes the extracellular N terminus of DuoxA1, was obtained from Santa Cruz Biotechnology, Inc. Unfortunately, no commercial Ab against DuoxA2 for immunoblotting or immunostaining is available. mAbs against HA(TANA2)-conjugated HRP, Alexa Fluor 488, and magnetic agarose were obtained from MBL International Corp. An mAb against FLAG(M2)-conjugated HRP was obtained from Sigma. Endoglycosidase H (Endo H) was obtained from New England Biolabs.

Cell Culture—HEK293 cells (ATCC) were maintained in Eagle's minimal essential medium (Wako Pure Chemical Industries) containing 10% FBS (Nichirei Biosciences), 100 μM nonessential aa (Wako Pure Chemical Industries), and antibiotics at 37 °C in 5% CO_2.

Construction of Plasmids—We used human Duox2, DuoxA1(α), and DuoxA2 in pcDNA3.1 (Invitrogen), which were previously described (7). Human Duox1 cDNA was a kind gift from Dr. Francoise Miot (Université Libre de Bruxelles, Brussels, Belgium) (4) and was transferred into pcDNA3.1. Duox1 and Duox2 with a 2×HA tag between Asn-23 and Pro-24 and between Asp-27 and Ala-28, respectively, in the first extracellular region were created in pcDNA3.1 by site-directed mutagenesis using a QuikChange Lightening Site-Directed Mutagenesis kit (Agilent Technologies). The chimeric construct Duox(1PoxH-2), possessing the PoxH domain of Duox1 (1–592 aa) and the Nox-like portion of Duox2 (596–1548 aa), and the chimeric construct Duox(2PoxH-1), possessing the PoxH domain of Duox2 (1–594 aa) and the Nox-like portion of Duox1 (592–1551 aa), were created in pcDNA3.1 by PCR and restriction enzyme-based recombination. DuoxA1 and DuoxA2 in both p3×FLAG-CMV-10 (Sigma) and p3×FLAG-CMV-14 (Sigma-Aldrich) vectors were made using PCR and named 3N×FLAG-DuoxA1, 3N×FLAG-DuoxA2, DuoxA1–3C×FLAG, and DuoxA2–3C×FLAG. DuoxA2 with 2×FLAG and DuoxA2 with 1×FLAG at the N terminus were made by QuikChange using 3N×FLAG-DuoxA2 as a template. DuoxA2 with 2×HA at the N terminus was made by QuikChange using DuoxA2 as a template. DuoxA1 with 1×FLAG at the C terminus was made by QuikChange using DuoxA1–3C×FLAG as a template. The chimeric construct DuoxA(1-2), possessing the N-terminal extracellular region of DuoxA1 (1–19 aa) and DuoxA2 (20–320 aa), and the chimeric construct DuoxA(2-1), possessing the N-terminal extracellular region of DuoxA2 (1–19 aa) and DuoxA1 (20–343 aa), were created in pcDNA3.1 using PCR. N-terminal deletion (2–17 aa) mutants of DuoxA1 and DuoxA2 were generated using PCR and named DuoxA1(N-del) and DuoxA2(N-del). All other mutants/chimeric constructs of Duox and DuoxA, including Duox2→1(A:8aa), Duox2→1(C:10aa), Duox2→1(E:TY/RF), Duox1→2(A:8aa+L), Duox1→Nox1(A), Duox1→Nox5(A), Duox2→Nox1(A), Duox2→Nox5(A), DuoxA-(1F-2), and DuoxA(2-1S-2), were made by QuikChange. These are named and described in Table 1 and are illustrated in Figs. 3*A*, 4*A*, 5*A*, 7*A*, 7*C*, and 8*A*. All plasmids were sequenced to confirm their identities.

In Vitro Binding (Pulldown) Assays—Forward and reverse oligonucleotides for DuoxA N terminus (1–20 aa for DuoxA1 or 1–19 aa for DuoxA2) were annealed and cloned into the BamHI and EcoRI sites of pGEX-6P-1. Purified GST and GST-tagged DuoxA N-terminal proteins (DuoxA1(N), GST-MATL-GHTFPFYAGPKPTFP; DuoxA2(N), GST-MTLWNGVLPF-YPQPRHAAG) were obtained as described previously (27). Biotin-labeled Duox A-loop peptides (Duox1(Aloop), biotin-AAHHTGITDTTRV; Duox2(Aloop), biotin-ALPPSDIAQT-TLV) were synthesized by MBL International. GST-tagged DuoxA(N) was mixed with biotin-labeled Duox(Aloop) in 300 μl of binding buffer (500 nM each) (27). After rotation for 2 h at 4 °C, 40 μl of streptavidin-coupled magnetic beads (Dynabeads M-280 Streptavidin; Invitrogen) were added to the solution, and the mixture was agitated for 90 min at 4 °C. The precipitates were washed 3 times using a magnetic rack, and then the material absorbed to the beads was eluted in Laemmli sample buffer; the magnetic beads were then removed using a magnetic rack. The eluents were subjected to SDS-PAGE followed by immunoblotting using a polyclonal antibody against GST (Santa Cruz Biotechnology). Bound antibodies were detected with an HRP-conjugated secondary antibody using the ECL detection system (GE Healthcare).

Immunoprecipitation and Immunoblotting—Various pairs of 2×HA-Duox and FLAG-tagged DuoxA constructs were co-transfected into HEK293 cells plated on 10-cm dishes using FuGENE 6 (Promega). Forty-eight hours after transfection, the cells were lysed in 250 μl of lysis buffer with a protease inhibitor mixture (27) by sonication. Total cell lysates were centrifuged at 800 × *g* for 5 min at 4 °C, and the supernatants were incubated with 10 μl of magnetic agarose-conjugated HA mAb for 2 h at 4 °C. The precipitates were washed 3 times, and aliquots of the precipitates were subjected to SDS-PAGE followed by immunoblotting using an HRP-conjugated FLAG mAb and detected using the ECL detection system.

N-Deglycosylation Analysis—The deglycosylation assay was performed as previously described (7). Briefly, various pairs of 2×HA-Duox and DuoxA constructs were co-transfected into HEK293 cells plated in 10-cm dishes using FuGENE 6. Forty-eight hours after transfection, the cells were lysed in 250 μl of lysis buffer with a protease inhibitor mixture. After centrifugation at 12,000 × *g* for 10 min at 4 °C, equal amounts of proteins were treated with 100 units/50 μl of Endo H for 30 min at 37 °C or left untreated and separated by SDS-PAGE. Immunoblotting was performed using an HRP-conjugated HA mAb.

Confocal Fluorescence Imaging Studies—A total of 2.5×10^5 HEK293 cells were seeded in 35-mm glass-bottomed dishes (MatTek Corp.) 48 h before transfection and transfected using FuGENE 6. Thirty-two hours after transfection, the cells were fixed using 4% paraformaldehyde in 0.1 M PBS (pH 7.4) without permeabilization and stained using an Alexa Fluor 488-conjugated HA mAb (1:500) at room temperature for 2 h for visualization by confocal laser scanning fluorescence microscopy (LSM700; Carl Zeiss AG). All imaging experiments were performed in triplicate and were repeated in at least three independent transfection experiments ($n \geq 9$).

ROS Production Assay—HEK293 cells were seeded in 6-well dishes at 2.5×10^5 cells/well 48 h before transfection. HEK293 cells were transfected using FuGENE 6 in complexes with various combinations of plasmids. The cells were fed 6 h post-transfection with complete medium and harvested using 0.02% EDTA solution (Nacalai Tesque). Thirty-two hours after transfection, 2×10^5 cells in Hank's balanced salt solution (HBSS(−); Wako Pure Chemical Industries) were used for ROS assays with 0.2 μM ionomycin (Sigma) + 2 mM Ca^{2+}. Chemiluminescence methods were used in the presence of luminol + HRP (Sigma) for gross ROS detection (H_2O_2, O_2^-, and other non-identified ROS), superoxide dismutase-inhibitable Diogenes reagent (National Diagnostics) for O_2^- detection, or Amplex Red (Invitrogen) + HRP for H_2O_2 detection for 10 min using a luminometer (Mithras LB940; Berthold Detection Systems GmbH) (28) as previously described (7, 29). O_2^- production from 5×10^5 cells in 100 μl of HBSS(−) stimulated by 0.2 μM ionomycin + 2 mM Ca^{2+} was also measured based on the assay of cytochrome *c* (100 μM, Sigma) reduction with a molar extinction coefficient of 21 mM^{-1} cm^{-1} at 550 nm using a monochrometer (Multiskan GO; Thermo Fisher Scientific) as previously described (7, 30). O_2^- production was inhibited by the addition of 10 units/ml superoxide dismutase (Sigma) in the assay solution. Comparable expression of proteins was confirmed by immunoblotting using total lysates from the same number of cells. Mean oxidase activities were calculated from at least three independent transfection experiments.

Statistical Analysis—All data are presented as the means ± S.E. of mean. For comparisons of more than two groups, one-way analysis of variance was performed. Statistical analyses were performed using GraphPad Prism 5.0 software (GraphPad Software Inc.); $p < 0.05$ was considered statistically significant.

RESULTS

Tags at the N terminus of DuoxA2 Enhance O_2^- Leakage from Matched Duox2-DuoxA2 Complexes—We previously demonstrated that co-expression of the mismatched Duox2 and DuoxA1, but not of Duox1 and DuoxA2, causes O_2^- leakage into the extracellular milieu (7). In this study we found that co-expression of matched Duox2 and DuoxA2, but not of Duox1 and DuoxA1, caused a small amount of O_2^- release (5.4 ± 0.6%) detected by Diogenes; this is consistent with the result of a previous report (31). To elucidate why only Duox2- and not Duox1-based combinations cause extracellular O_2^- release, we created a series of N-terminally FLAG-tagged DuoxA1 and DuoxA2 constructs (Table 1). Interestingly, although C-terminally 3×FLAG-tagged DuoxA2 co-expressed with Duox2 did

TABLE 1

Summary of the Duox and DuoxA expression constructs used

PoxH, peroxidase homology; F, first half; S, second half; N, N terminus; C, C terminus; A, A-loop; C, C-loop; E, E-loop; FLAG-tagged constructs are in p3×FLAG-CMV vector and all other constructs in pcDNA3.1.

Name of protein	Structures of expressed protein
Duox	
Duox1 and Duox2	Wild type Duox1 and Duox2
2×HA-Duox1	2 × HA tag between Asn-23 and Pro-24 of extracellular PoxH domain
2×HA-Duox2	2 × HA tag between Asp-27 and Ala-28 of extracellular PoxH domain
Duox PoxH-domain chimera	
Duox(1PoxH-2)	Chimera of PoxH domain of Duox1 (1–592 aa) and Nox-like portion of Duox2 (596–1548 aa)
Duox(2PoxH-1)	Chimera of PH domain of Duox2 (1–594 aa) and Nox-like portion of Duox1 (592–1551 aa)
DuoxA	
DuoxA1 and DuoxA2	Wild type DuoxA1 and DuoxA2
3NxFLAG-DuoxA1	3xFLAG tag at the extracellular N terminus
DuoxA1–3CxFLAG	3xFLAG tag at the intracellular C terminus
DuoxA1–1CxFLAG	1xFLAG tag at the extracellular C-terminus
DuoxA1(N-del)	The extracellular N terminus (2–17 aa) deletion
3NxFLAG-DuoxA2	3xFLAG tag at the extracellular N terminus
2NxFLAG-DuoxA2	2 × FLAG tag at the extracellular N terminus
1NxFLAG-DuoxA2	1xFLAG tag at the extracellular N terminus
2NxHA-DuoxA2	2 × HA tag at the extracellular N terminus
DuoxA2–3CxFLAG	3xFLAG tag at the intracellular C terminus
DuoxA2(N-del)	The extracellular N terminus (2–17 aa) deletion
DuoxA N-terminal chimera	
DuoxA(1–2)	Chimera of extracellular N terminus of DuoxA1 (1–19 aa) and DuoxA2 (20–320 aa)
DuoxA(2–1)	Chimera of extracellular N terminus of DuoxA2 (1–19 aa) and DuoxA1 (20–343 aa)
DuoxA(1F-2)	Chimera of DuoxA1 (1–8 aa; first half of 19aa) and DuoxA2 (9–320 aa)
DuoxA(2–1S-2)	Chimera of DuoxA2 (1–11 aa), DuoxA1 (12–19 aa; second half of 19aa), and DuoxA2 (20–320 aa)
A-loop	
Duox2→1(A:5aa)	5aa in A-loop of Duox2 is replaced by corresponding 5aa in A-loop of Duox1
Duox2→1(A:8aa)	8aa in A-loop of Duox2 is replaced by corresponding 8aa in A-loop of Duox1
Duox1→2(A:F4aa)	4aa (first half of 8aa) in A-loop of Duox1 is replaced by corresponding 4aa in A-loop of Duox2
Duox1→2(A:S4aa)	4aa (second half of 8aa) in A-loop of Duox1 is replaced by corresponding 4aa in A-loop of Duox2
Duox1→2(A:8aa)	8aa in A-loop of Duox1 replaced by corresponding 8aa in A-loop of Duox2
Duox1→2(A:8aa+L)	8aa + Arg in A-loop of Duox1 replaced by corresponding residues (8aa + Leu) in A-loop of Duox2
Duox1→2(A:8aa+GL)	8aa + Ala and Arg in A-loop of Duox1 replaced by corresponding residues (8aa + Gly and Leu) in A-loop of Duox2
Duox1→2(A:8aa+L)+L/A	Duox1→2 (A:8aa + L) with reversed mutation (Duox2 to Duox1), Leu to Ala
Duox1→2(A:8aa+L)+PP/HH	Duox1→2 (A:8aa + L) with reversed mutation (Duox2 to Duox1), Pro-Pro to His-His
Duox1→2(A:8aa+L)+PP/HP	Duox1→2 (A:8aa + L) with reversed mutation (Duox2 to Duox1), Pro-Pro to His-Pro
Duox1→2(A:8aa+L)+PP/PH	Duox1→2 (A:8aa + L) with reversed mutation (Duox2 to Duox1), Pro-Pro to Pro-His
Duox1→2(A:8aa+L)+D/G	Duox1→2 (A:8aa + L) with reversed mutation (Duox2 to Duox1), Asp to Gly
Duox1→2(A:8aa+L)+A/T	Duox1→2 (A:8aa + L) with reversed mutation (Duox2 to Duox1), Ala to Thr
Duox1→2(A:8aa+L)+Q/D	Duox1→2 (A:8aa + L) with reversed mutation (Duox2 to Duox1), Gln to Asp
Duox1→2(A:PPD)	3aa residues in A-loop of Duox1 are replaced by corresponding Pro,Pro and Asp residues in A-loop of Duox2
Duox-Nox(A-loop) chimera	
Duox1→Nox1(A)	7aa in A-loop of Duox1 replaced by corresponding residues in A-loop of Nox1
Duox1→Nox5(A)	7aa in A-loop of Duox1 replaced by corresponding residues in A-loop of Nox5
Duox2→Nox1(A)	7aa in A-loop of Duox2 replaced by corresponding residues in A-loop of Nox1
Duox2→Nox5(A)	7aa in A-loop of Duox2 replaced by corresponding residues in A-loop of Nox5
C-loop	
Duox2→1(C:10aa)	10aa (IVLAINVVNK) in C-loop of Duox2 replaced by corresponding 10 aa in C-loop of Duox1 (LIVSLGLHDE)
E-loop	
Duox2→1(E:TY/RF)	Thr and Tyr in E-loop of Duox2 replaced by corresponding Arg and Phe in E-loop of Duox1

not enhance O_2^- release, N-terminally tagged DuoxA2 dramatically enhanced the amount of O_2^- release regardless of the number or type of epitope tags (Fig. 2*A*; 3N×FLAG, 291.2 ± 36.5%; 2N×FLAG, 387.4 ± 9.1%; 1N×FLAG, 543.9 ± 66.9%; 2N×HA, 465.4 ± 67.8%). Duox1 exhibited no O_2^- leakage when co-expressed in any combination regardless of whether DuoxA was untagged, N-terminally 3×FLAG-tagged, or C-terminally 3×FLAG-tagged (Fig. 2*A*; data not shown). O_2^- release by Duox2 with DuoxA1 or various types of N-terminally tagged DuoxA2 was confirmed by examining the effect of superoxide dismutase and/or through cytochrome *c* reduction assays (Fig. 2, *A* and *B*). The luminol + HRP assays were used to detect gross ROS production (H_2O_2, O_2^-, and other non-identified ROS) and to measure the ROS production capabilities in each Duox-DuoxA pair. Immunoblotting was performed to confirm comparable expression of constructs used (Fig. 2*C*). The results of these assays suggested that altered interactions between Duox2 and the N-terminal regions of its maturation factor, DuoxA2, cause increased O_2^- leakage from this enzyme complex; the same was not observed in case of Duox1.

The N-terminal Extracellular Region of DuoxA1 Plays a Pivotal Role in O_2^- Release—DuoxA proteins have four TM segments, and their N-terminal regions are positioned on the extracytoplasmic membrane surface (6). When transported to the plasma membrane in complexes with Duoxes, the N termini of DuoxA proteins are detectable on the cell surface (7). To confirm the importance of the N-terminal extracellular regions of DuoxAs for O_2^- leakage, we made two chimeric mutants of DuoxA1 and DuoxA2: DuoxA(1-2), in which the N-terminal extracellular region of DuoxA2 was substituted with that of DuoxA1, and DuoxA(2-1), in which the N-terminal extracellular region of DuoxA1 was substituted with that of DuoxA2 (Fig.

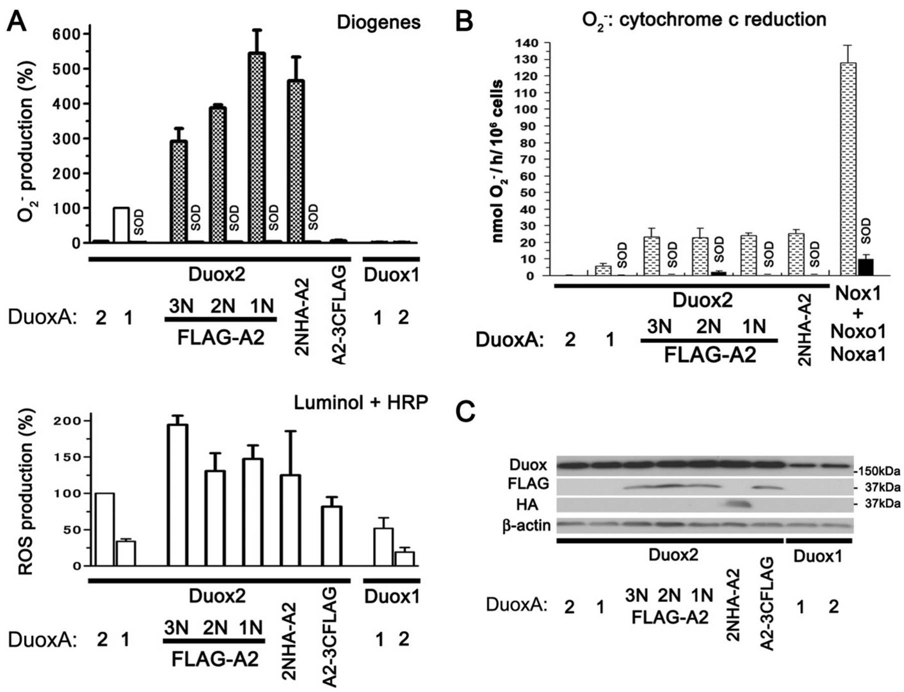

FIGURE 2. **O_2^- leakage from Duox2 paired with N-terminally tagged DuoxA2.** *A*, Various Duox and DuoxA pairs were transfected into HEK293 cells. O_2^- and reactive oxygen species were measured by chemiluminescence assay using Diogenes and luminol + HRP, respectively. Duox2 + various types of N-terminally, but not C-terminally, tagged DuoxA2, show enhanced O_2^- production. The superoxide dismutase (*SOD*) treatment was performed to validate the O_2^- production for those samples where marked O_2^- production was observed. *B*, various Duox and DuoxA pairs were transfected into HEK293 cells, and O_2^- was measured by cytochrome *c* reduction assay. NADPH oxidase 1-based O_2^- production was used as a positive control. All the samples were subjected to the superoxide dismutase treatment, except for Duox2-DuoxA2. *C*, immunoblotting detects expression levels of Duox2 and Duox1 in various pairs as well as the expression of FLAG- and HA-tagged DuoxAs.

3*A*). When co-expressed with DuoxA(2-1), Duox2 exhibited no O_2^- release (Fig. 3*B*); in contrast, when co-expressed with DuoxA(1-2), Duox2 showed markedly enhanced O_2^- release (Fig. 3*B*). To define the specific aa sequence in the N-terminal extracellular region of DuoxA(1-2) that influences O_2^- release, we made two additional chimeric mutants of DuoxA(1-2): DuoxA(1F-2), in which only the first half of the N-terminal extracellular region of DuoxA2 was substituted with that of DuoxA1, and DuoxA(2-1S-2), in which only the second half of the N-terminal extracellular region of DuoxA2 was substituted with that of DuoxA1 (Fig. 3*A*). O_2^- release from Duox2 with DuoxA(1F-2) or DuoxA(2-1S-2) was similar, at about one-third that from Duox2 + DuoxA(1-2) (Fig. 3*B*). Duox1 with DuoxA(2-1) or DuoxA(1-2) showed no O_2^- release (Fig. 3*B*). Comparable expression of constructs was confirmed by immunoblotting (Fig. 3*B*). DuoxA1 pAb detected only WT DuoxA1 and not DuoxA1 chimeras. These results suggest that the entire N-terminal, extracellular region of DuoxA1 has a strong influence on O_2^- release when expressed in combination with Duox2.

The Extracellular Region(s) after the First TM Segment of Duox2 Is Key to O_2^- Release—To explore the regions of Duox involved in O_2^- release, we made two chimeric Duox mutants: Duox(2PoxH-1), in which PoxH domain of Duox1 was substituted with that of Duox2, and Duox(1PoxH-2), in which the PoxH domain of Duox2 was substituted with that of Duox1 (Fig. 4*A*). Three combinations, Duox2-DuoxA1, Duox(1PoxH-2)-DuoxA1, and Duox(1PoxH-2)-DuoxA(1-2) (highlighted by *two-way red arrows* in Fig. 4*B*), showed O_2^- release. All these combinations contained the common Duox2 portion starting with the first TM segment and the N-terminal extracellular region of DuoxA1. Comparable expression of constructs was confirmed by immunoblotting (Fig. 4*B*). These results suggest that the extracellular region(s) after the first TM segment of Duox2 and the N-terminal extracellular region of DuoxA1 affect O_2^- leakage.

The A-loops of Duoxes, but Not the C- or E-loops, Affect O_2^- Release—To identify the extracellular region after the first TM segment of Duox2 involved in O_2^- release in cooperation with the N-terminal extracellular region of DuoxA1, we focused on three extracellular regions of Duoxes, A-, C-, and E-loop (Fig. 1*A*). Because Duoxes, like all Nox enzymes, donate electrons to molecular oxygen in the extracytoplasmic compartment, we did not examine the roles of the intracellular EF-hand motifs or the B- or D-loops in O_2^- release. These loops were defined in reference to previous papers (4, 23) and using websites that predict the secondary structures of membrane proteins (SOSUI WWW Server; TMHMM Server). We hypothesized that if a particular extracellular loop of Duox2 was involved in O_2^- release, then chimeric mutants in which this loop of Duox2 is replaced with that of Duox1 would exhibit reduced O_2^- leakage. To explore this hypothesis, we first made two chimeric mutants of Duox2 possessing the A-loop sequences of Duox1: Duox2→1(A:5aa) and Duox2→1(A:8aa) (Fig. 5*A*). O_2^- release by Duox2→1(A:5aa)-DuoxA1 and Duox2→1(A:8aa)-DuoxA1 was dramatically reduced relative to the Duox2-DuoxA1 complex (2.27 ± 0.81% and 0.83 ± 0.38%, respectively; Fig. 5*B*). To confirm these results, we made three reverted chimeric mutants of Duox1 possessing some A-loop sequence

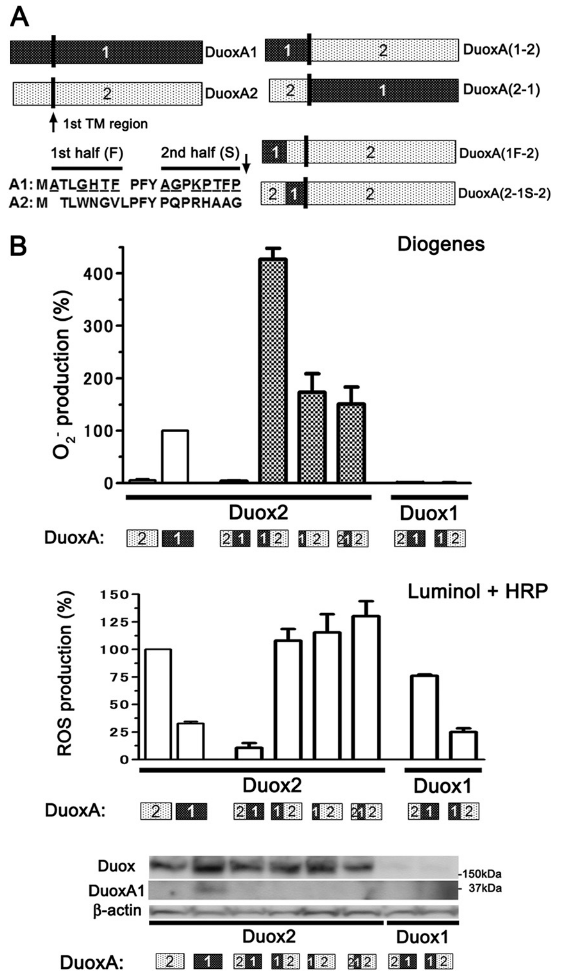

FIGURE 3. **$O_2^{\cdot-}$ leakage from Duox2 paired with DuoxAs with the N-terminal extracellular region of DuoxA1.** *A*, illustration showing DuoxA1, DuoxA2, and four chimeric DuoxA proteins: DuoxA(1-2), DuoxA(2-1), DuoxA(1F-2), and DuoxA(2-1S-2). *B*, various Duox and DuoxA pairs were transfected into HEK293 cells. $O_2^{\cdot-}$, and reactive oxygen species were measured by chemiluminescence assay using Diogenes and luminol + HRP, respectively. Duox2 + DuoxAs with the N-terminal extracellular region of DuoxA1 show $O_2^{\cdot-}$ production in the following order: DuoxA(1-2) > DuoxA(1F-2) = DuoxA(2-1S-2). Immunoblotting detected the expression of Duoxes and DuoxAs. A pAb against Duoxes preferentially reacts with Duox2 via its first intracellular loop but also faintly detects Duox1 (the last two lanes). A pAb for DuoxA1, which reacts with its extracellular N terminus, only detects wild-type DuoxA1.

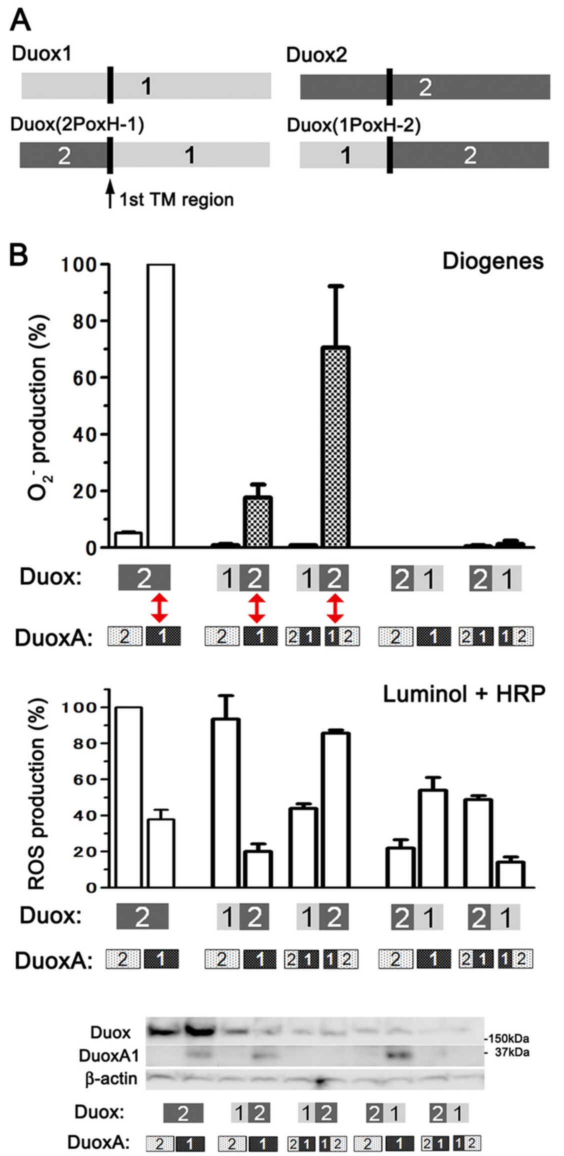

FIGURE 4. **$O_2^{\cdot-}$ leakage from pairs of Duoxes with the Nox-like portion of Duox2 and DuoxAs with the N-terminal extracellular region of DuoxA1.** A, illustration showing Duox1, Duox2, and two chimeric Duox proteins: Duox(1PoxH-2) and Duox(2PoxH-1). *B*, various Duox and DuoxA pairs were transfected into HEK293 cells. $O_2^{\cdot-}$ and total reactive oxygen species were measured by chemiluminescence assay using Diogenes and luminol + HRP, respectively. Pairs (*red arrows*) with the Duox2 portion after the first transmembrane segment (termed the Nox-like portion) + DuoxA with the N-terminal extracellular region of DuoxA1 show $O_2^{\cdot-}$ production. Immunoblotting detects the expression levels of various Duox and DuoxA pairs. A pAb against Duoxes faintly detected Duox2 chimeras in the *two right-hand lanes*. A pAb for DuoxA1 detects only wild-type DuoxA1.

from Duox2: Duox1→2(A:F4aa), Duox1→2(A:S4aa), and Duox1→2(A:8aa) (Fig. 5*A*). Although Duox1→2(A:F4aa) and Duox1→2(A:S4aa) showed no $O_2^{\cdot-}$ release, Duox1→2(A:8aa) co-expressed with DuoxA1 did show $O_2^{\cdot-}$ release (67.4 ± 8.9%) but to a lesser extent than that by Duox2-DuoxA1 (Fig. 5*B*). Duox1→2(A:8aa) maintained capabilities to secret H_2O_2, which were detected by Amplex Red + HRP, as in the case of Duox1 and Duox2 (Fig. 5*B*). We then made two additional Duox1 mutants: Duox1→2(A:8aa+L) and Duox1→2(A:8aa+GL) (Table 1). In Duox1→2(A:8aa+GL), the entire A-loop aa sequence of Duox1 was replaced with that of Duox2. $O_2^{\cdot-}$ release from Duox1→2(A:8aa+L)-DuoxA1 (146.9 ± 16.7%) and Duox1→2(A:8aa+GL)-DuoxA1 (101.4 ± 19.3%) matched that from Duox2-DuoxA1 (Fig. 5*C*); therefore, Duox1→2(A:8aa+L) was used for further studies.

To examine which aa residues in the A-loop of Duox1 are critical for the reduction of $O_2^{\cdot-}$ release, we made various mutants in which one or two aa residues in the A-loop of Duox1→2(A:8aa+L) were reverted to those of Duox1. Changing Pro^{1068}-Pro^{1069} into His-His (PP/HH) and Asp^{1071} into Gly (D/G) almost completely abolished $O_2^{\cdot-}$ release (ROS production detected by luminol + HRP was 57.4 ± 8.3% and 54.9 ± 6.9%, respectively). In contrast, changing Leu^{1067} into Ala (L/A), Ala^{1073} into Thr (A/T), and Gln^{1074} into Asp (Q/D) caused moderate effects. Replacement of either Pro residue with His was sufficient to abolish $O_2^{\cdot-}$ release by Duox1→2(A:

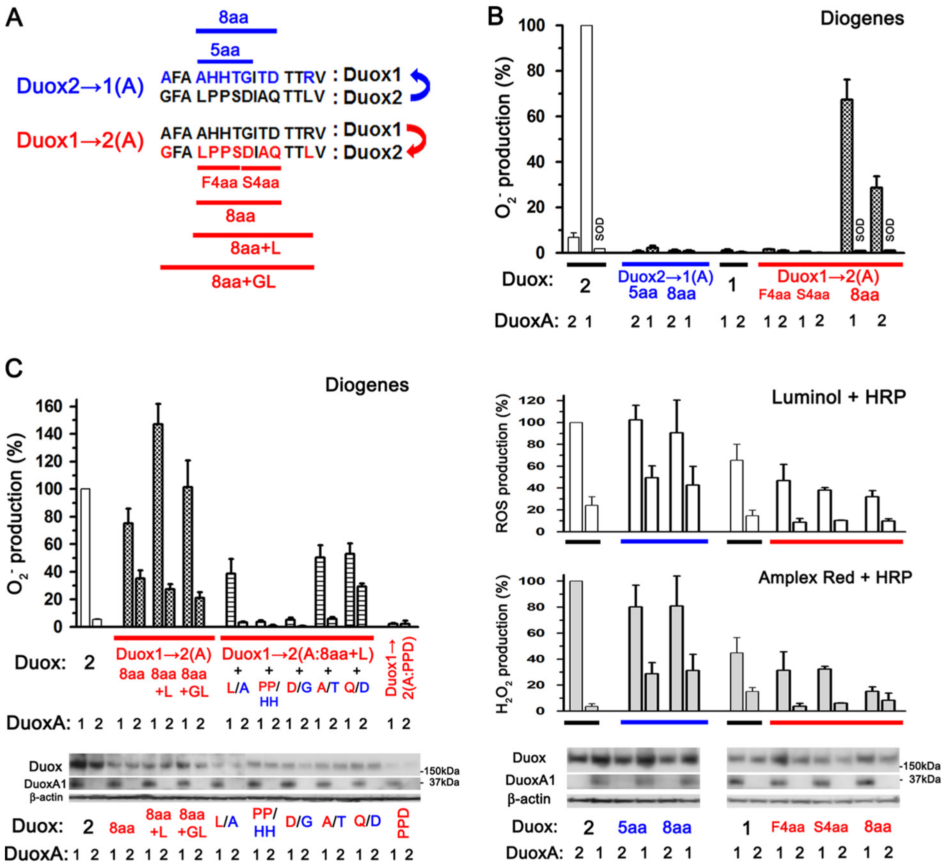

FIGURE 5. **The A-loop of Duox is associated with O_2^- leakage.** *A*, alignment of the A-loops of Duox1 and Duox2. The upper (*blue*) and lower (*red*) illustrations indicate the changes in aa sequence (number and residue) of the A-loop from Duox2 to Duox1 (*Duox2→1(A)*) and those from Duox1 to Duox2 (*Duox1→2(A)*), respectively. *B*, various pairs, including Duox2→1(A:5aa) or Duox2→1(A:8aa) + DuoxA, Duox1→2(A:F4aa), Duox1→2(A:S4aa), or Duox1→2(A:8aa) + DuoxA, were transfected into HEK293 cells. O_2^-, reactive oxygen species, and H_2O_2 were measured by chemiluminescence assay using Diogenes, luminol + HRP, and Amplex Red + HRP, respectively. Neither Duox2→1(A:5aa) nor Duox2→1(A:8aa) shows significant O_2^- production. In contrast, Duox1→2(A:8aa), but not Duox1→2(A:F4aa) or Duox1→2(A:S4aa), gained the ability to produce O_2^-, which is abolished by the addition of superoxide dismutase. Immunoblotting detects comparable expression levels of various Duox and DuoxA pairs. *C*, various pairs of Duox1→2(A) + DuoxA were transfected into HEK293 cells. O_2^- was measured by chemiluminescence assay using Diogenes. Duox1→(A:8aa+L) + DuoxA1 shows the highest O_2^- production. PP/HH or D/G mutations abolish O_2^- production by Duox1→2(A:8aa+L). Duox1→2(A:PPD) + DuoxA shows no ability to produce O_2^-. Immunoblotting detects expression levels of various Duox and DuoxA pairs.

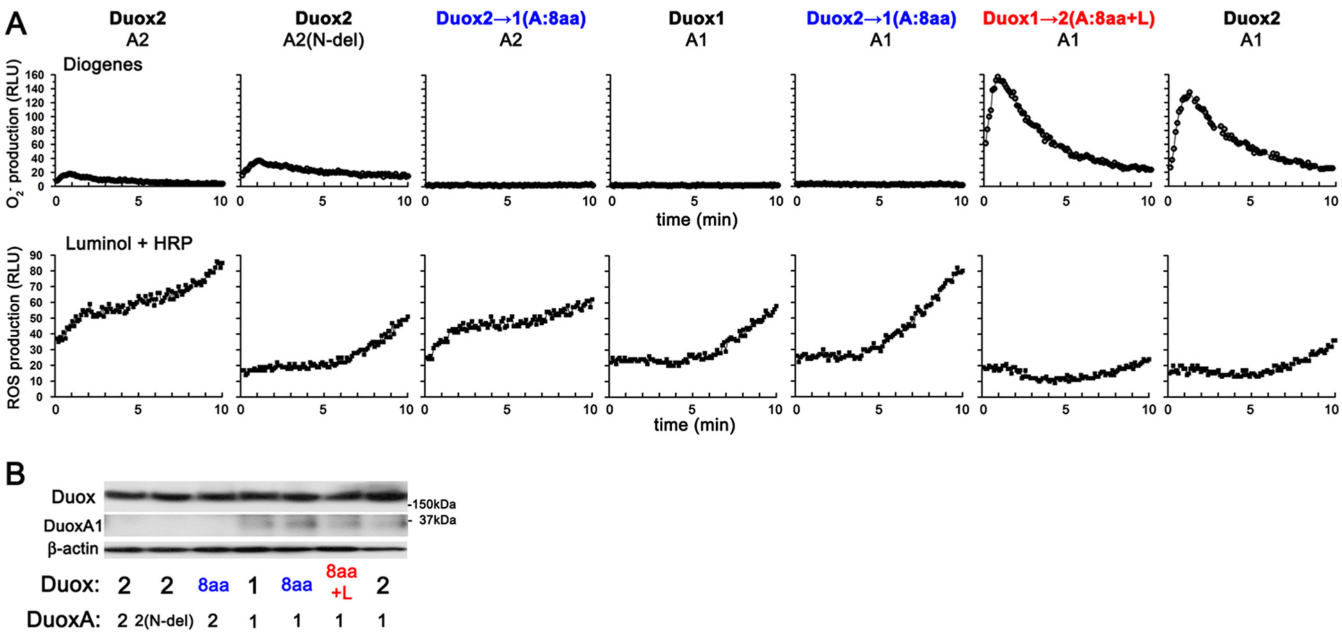

FIGURE 6. **Kinetics of O_2^- and ROS production.** *A*, various pairs, including HA-Duox2-DuoxA2, HA-Duox2-DuoxA2(N-del), HA-Duox2→1(A:8aa)-DuoxA2, HA-Duox1-DuoxA1, HA-Duox2→1(A:8aa)-DuoxA1, HA-Duox1→2(A:8aa+L)-DuoxA1, and HA-Duox2-DuoxA1, were transfected into HEK293 cells. Representative ($n \geq 3$) kinetics of O_2^- and reactive oxygen species production measured by chemiluminescence assay using Diogenes and luminol + HRP, respectively, are shown. *B*, immunoblotting detects comparable expression levels of various Duox and DuoxA pairs.

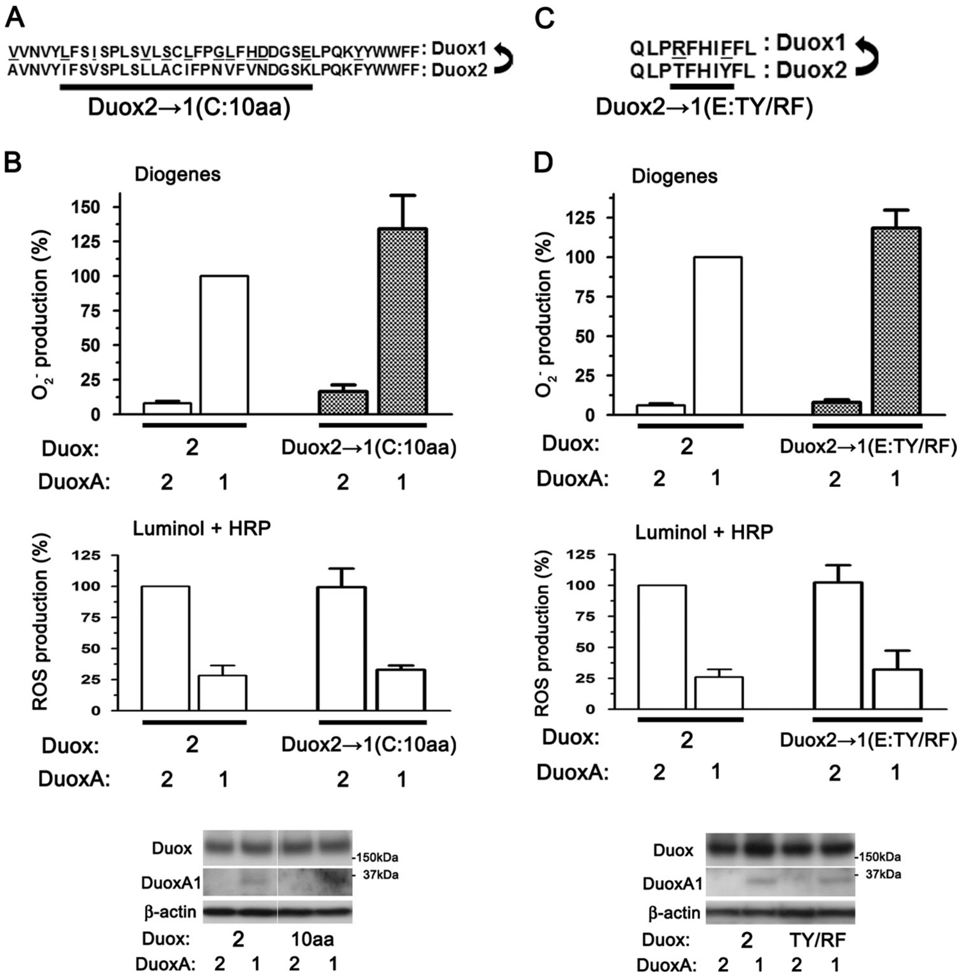

FIGURE 7. **The C- and E-loop of Duox are not associated with O_2^- leakage.** *A*, alignment of the C-loops of Duox1 and Duox2 and illustrations of chimeric Duox2 mutants indicating the residue and number of amino acids changes in the C-loop from Duox2 to Duox1 (Duox2→1(C)). *B*, Duox2→1(C:10aa) and DuoxA pairs were transfected into HEK293 cells. O_2^- and ROS were measured by chemiluminescence assays using Diogenes and luminol + HRP, respectively. The Duox2→1(C:10aa) + DuoxA pairs show no decreased O_2^- production. Immunoblotting (from the same membrane and image) detects comparable expression levels of various Duox and DuoxA pairs. *C*, alignment of the E-loops of Duox1 and Duox2 and illustrations of chimeric Duox2 mutants indicating the residues change in the E-loops from Duox2 to Duox1 (Duox2→1(E)). *D*, Duox2→1(E:TY/RF) and DuoxAs pairs were transfected into HEK293 cells. O_2^- and ROS were measured by chemiluminescence assay using Diogenes and luminol + HRP, respectively. The Duox2→1(E:TY/RF) + DuoxA pairs show no decreased O_2^- production. Immunoblotting detects comparable expression levels of various Duox and DuoxA pairs.

8aa+L); this was confirmed using PP/HP and PP/PH mutations in Duox1→2(A:8aa+L) (data not shown). In addition, although the expression levels of Duox1→2(A:PPD), in which three critical residues (HH+G) in the A-loop of Duox1 were exchanged for those of Duox2, were apparently low (ROS production detected by luminol + HRP was 36.8 ± 10.8%), it showed no O_2^- release (Fig. 5*C*). Taken together, these results suggest that these specific residues alone do not account for the function of the Duox A-loop in preventing O_2^- release. Comparable expression of constructs was confirmed by immunoblotting (Fig. 5, *B* and *C*).

Next, we examined the kinetics of O_2^- and ROS production (detected by Diogenes and luminol + HRP, respectively) from various Duox + DuoxA pairs: Duox2-DuoxA2, Duox2-DuoxA2(N-del), Duox2→1(A:8aa)-DuoxA2, Duox1-DuoxA1, Duox2→1(A:8aa)-DuoxA1, Duox1→2(A:8aa+L)-DuoxA1, and Duox2-DuoxA1. Duox1→2(A:8aa+L)-DuoxA1 and Duox2-DuoxA1 showed very similar kinetic curves in terms of both O_2^- and ROS production (Fig. 6*A*). Duox2→1(A:8aa)-DuoxA1 showed a kinetic curve of ROS production similar to that of Duox1-DuoxA1 (Fig. 6*A*). Duox2-DuoxA2(N-del) showed an increase in O_2^- release and a decrease in ROS production compared with Duox2-DuoxA2 (Fig. 6*A*). Duox2→1(A:8aa+L)-DuoxA2 did not show any O_2^- release (Fig. 6*A*). In the Duox1-DuoxA1(N-del) pair, ROS production was severely impaired (<10% that of Duox1-DuoxA1), and no apparent plasma membrane targeting/localization of Duox1 or O_2^- release was observed (data not shown). Comparable expression of constructs was confirmed by immunoblotting (Fig. 6*B*).

Finally, we assessed the involvement of the C- and E-loops in O_2^- release using chimeric mutants in which their sequences in Duox2 were replaced with those of Duox1 (Fig. 7, *A* and *C*). O_2^- release was not reduced in either the C-loop mutant, Duox2→1(C:10aa), or the E-loop mutant, Duox2→1(E:TY/RF) (Fig. 7, *B* and *D*). Comparable expression of constructs was confirmed by immunoblotting (Fig. 7, *B* and *D*). Taken together, we conclude that the A-loop, but not the C- or E-loop, of Duox2 is involved in O_2^- release.

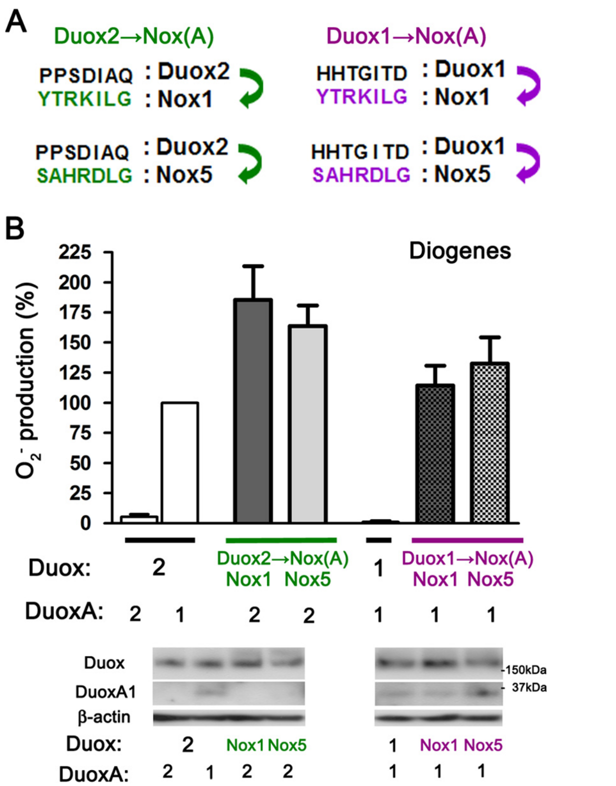

FIGURE 8. **The A-loops of both Duox1 and Duox2 prevent O_2^- leakage.** The illustrations indicate changes in the core aa sequences of the A-loops (7 aa) from Duoxes to Nox (1 or 5). *Green* and *purple* colors indicate the changes from Duox2 to Nox1 or Nox5 (Duox2→Nox(A)) and those from Duox1 to Nox1 or Nox5 (Duox1→Nox(A)), respectively. Various pairs were transfected into HEK293 cells. O_2^- was measured by a chemiluminescence assay using Diogenes. Immunoblotting detects comparable expression levels of various Duox and DuoxA pairs.

The A-loops of Both Duox1 and Duox2 Function in Reducing O_2^- Leakage—To further investigate the mechanism underlying the reduction of O_2^- release by the Duox A-loop, we made chimeric Duox proteins possessing the A-loops of Nox1 or Nox5 (23, 32) (Fig. 8*A*). Duox2 possessing the A-loop of Nox1 or Nox5 showed markedly enhanced O_2^- release in matched combination with DuoxA2 in comparison with the native Duox2-DuoxA2 complex (Fig. 8*B*), suggesting that the A-loop of Duox2 also functions in the reduction of O_2^- release. Furthermore, Duox1 possessing the A-loop of Nox1 or Nox5 exhibited O_2^- release even when matched with DuoxA1 (Fig. 8*B*). Comparable expression of constructs was confirmed by immunoblotting (Fig. 8*B*). Taken together, these observations imply that the A-loops of both Duox1 and Duox2 function in reducing O_2^- release, although it appears that the A-loop of Duox1 is more effective in reducing O_2^- release.

Stable and Mature Duox-DuoxA Complex Formation Is Required for H_2O_2 Production—To examine the hypothesis that the A-loops of Duoxes have the intrinsic ability to convert O_2^- to H_2O_2, we synthesized oligopeptides of the A-loops of Duox1 and Duox2. We performed the following experiments: 1) adding A-loop peptides into xanthine oxidase reactions generating O_2^- to detect its conversion and 2) adding A-loop peptides into Diogenes-based O_2^- assays in heterologous Duox-reconstituted cell systems. However, these experiments failed to reduce O_2^- production (data not shown), suggesting that the A-loops of Duoxes have no O_2^- dismutation activity.

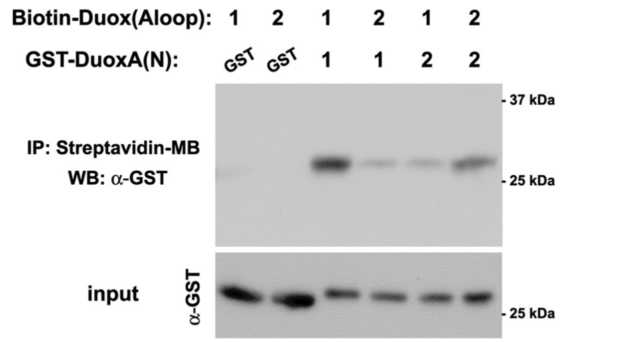

FIGURE 9. **Direct binding of the Duox A-loop to the DuoxA N terminus.** Purified GST-tagged DuoxA N terminus was mixed with synthesized biotin-labeled Duox A-loop in binding buffer. *IP*, immunoprecipitation. Then, streptavidin-coupled magnetic beads were added 2 h later. The material absorbed to the beads was eluted in Laemmli sample buffer. The eluents were subjected to SDS-PAGE followed by immunoblotting (*WB*) using a polyclonal antibody against GST. The strongest interaction was observed between Duox1(Aloop) and DuoxA1(N) relative to Duox2(Aloop) + DuoxA2(N), Duox1(Aloop) + DuoxA2(N), and Duox2(Aloop) + DuoxA1(N) ($n \geq 3$).

Next, we investigated possible direct interaction between the biotin-labeled A-loop peptides of Duoxes and the GST-tagged N-terminal extracellular sequences of the DuoxAs by pulldown assays using streptavidin-conjugated magnetic beads. We detected the strongest interaction between Duox1(Aloop) and DuoxA1(N) among Duox1(Aloop)-DuoxA1(N), Duox2(Aloop)-DuoxA2(N), Duox1(Aloop)-DuoxA2(N), and Duox2(Aloop)-DuoxA1(N) pairs (Fig. 9).

We then focused on the interaction between full-length Duoxes and DuoxAs at the cellular level because our previous paper established that Duox maturation, reflected in *N*-glycosyl modifications and stable interactions with DuoxAs, affects the type of ROS produced in that fully processed and stable complexes do not leak O_2^- (7). The relationship between O_2^- release and Duox binding to DuoxAs was examined by immunoprecipitation assays using lysates from HEK293 cells transfected with various Duox and DuoxA combinations. The order of the strength of Duox2 binding to FLAG-tagged DuoxAs was 3N×FLAG-DuoxA2 < DuoxA1–3C×FLAG < DuoxA2–3C×FLAG (Fig. 10*A*). This order inversely correlated with the amount of O_2^- release by the Duox2 complex: 3N×FLAG-DuoxA2 > DuoxA1–3C×FLAG > DuoxA2–3C×FLAG (Fig. 10*A*). The order of the strength of DuoxA1 binding to HA-tagged Duoxes was HA-Duox1→2(A:8aa+L) < HA-Duox2 < HA-Duox1 = HA-Duox2→1(A:8aa) (Fig. 10*B*). This order also inversely correlated with the amount of O_2^- release: HA-Duox1→2(A:8aa+ L) > HA-Duox2 > HA-Duox1 = HA-Duox2→1(A:8aa) (Fig. 10*B*), suggesting that stable interactions between Duoxes and DuoxAs prevent O_2^- release. Comparable plasma membrane targeting/localization of these seven pairs was statistically confirmed by the nonpermeable immunostaining of HA-tagged Duoxes using an Alexa Fluor 488-conjugated HA mAb (data not shown).

To explore the relationship between Duox maturation (Golgi apparatus-based glycosyl modifications) and O_2^- release, Endo H treatments were performed. Duox2-DuoxA1 complexes that showed O_2^- release was sensitive to Endo H treatment (Fig. 10*C*,

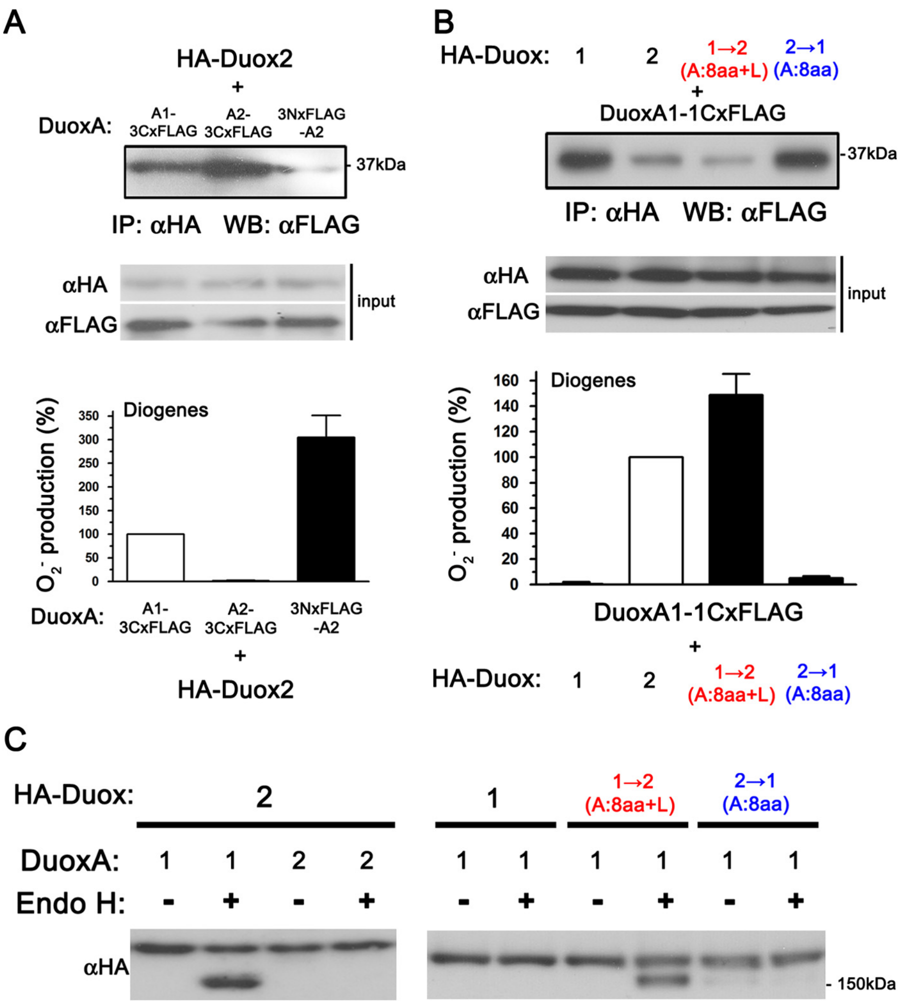

FIGURE 10. **The A-loop of Duox is associated with binding to DuoxA, $O_2^{\cdot-}$ leakage, and Endo H-resistant *N*-glycosyl modification.** *A* and *B*, HA-tagged Duox2 + various types of FLAG-tagged DuoxA (*A*) or various types of HA-Duox + DuoxA1–1C×FLAG (*B*) were transfected into HEK293 cell. Forty-eight hours after transfection lysates were immunoprecipitated (*IP*) by a magnetic agarose-conjugated HA mAb followed by immunoblotting (*WB*) using an HRP-conjugated FLAG mAb. Representative data ($n \geq 3$) show good correlation between a weak interaction between Duox and DuoxA and high $O_2^{\cdot-}$ production. *C*, various HA-tagged Duox and DuoxA pairs were transfected into HEK293 cell. Forty-eight hours after transfection lysates were treated with Endo H, and immunoblotting was performed using an HRP-conjugated HA mAb. Representative data ($n \geq 3$) show the presence of Endo H-sensitive bands in $O_2^{\cdot-}$ producing pairs (HA-Duox2 + DuoxA1 and HA-Duox1→2(A:8aa+L) + DuoxA1).

left). Interestingly, although the Duox1→2(A:8aa+L)-DuoxA1 complex showed glycosyl modifications of Duox1→2(A:8aa+L) similar to that of Duox1 in the Duox1-DuoxA1 complex, the Duox1→2(A:8aa+L)-DuoxA1 complex that exhibited $O_2^{\cdot-}$ release was also susceptible to Endo H treatment (Fig. 10*C*, *right*). Conversely, Duox2→1(A:8aa)-DuoxA1, which produced H_2O_2 but no $O_2^{\cdot-}$, was resistant to Endo H treatment (Fig. 10*C*, *right*). Taken together, these results suggest that the A-loop of Duox1 functions to promote the formation of stable and mature Duox1-DuoxA1 complexes, preventing $O_2^{\cdot-}$ release.

DISCUSSION

Duox enzymes serve as dedicated H_2O_2 generators at the plasma membrane, where they support the activities of extracellular hemoperoxidases (22). We (7) and another group (26) previously reported a switch in the type of ROS released, from H_2O_2 to $O_2^{\cdot-}$, with co-expression of the mismatched Duox2 and DuoxA1 pair, but not with Duox1 and DuoxA2 (7). These findings suggest that DuoxA proteins contribute to Duox maturation and subcellular targeting; they also function as a part of the ROS-generating complex. Subsequently, Hoste *et al.* (31) showed that the N terminus of DuoxA2 acts as an important determinant of the type of ROS produced by Duox2 by comparing native DuoxA2 with N-terminally truncated and chimeric versions of DuoxA2 and DuoxA1. Consistent with our results, they showed that 1) the addition of tags of various types and lengths to the N-terminal of DuoxA2 increased the amount of $O_2^{\cdot-}$ leakage by Duox2 (rhodopsin (19 aa) and FLAG (8 aa) tags (31); FLAG (22 aa in 3N×FLAG, 15 aa in 2N×FLAG, and 8 aa in 1N×FLAG), and 2N×HA (20 aa) tags (this study)) and 2) a small amount of $O_2^{\cdot-}$ is released by the native Duox2-DuoxA2 complex but not by the Duox1-DuoxA1 or Duox1-DuoxA2 complexes (31).

In this study we expanded upon these observations on ROS generation by Duoxes by identifying novel structural determinants within the Nox-like extracellular portion of Duoxes, termed the A-loop, that appears to function in preventing $O_2^{\cdot-}$ leakage by supporting the stabilization and maturation of the

Duox1	human	AFA AHHTGITD TTRV
	cow	AFA AHHKGIAD TTRV
	pig	AFA AHHTGIMD TTRV
	dog	AFA AHHTGIMD TTRV
	rat	AFA AHHTGISD TTRV
	mouse	AFA AHHTGISD TTRV
	frog	AFE SQHRGISE VTMP
Duox2	human	GFA LPPSDIAQ TTLV
	cow	AFA SPPSGIAQ TTFV
	pig	AFV SPPSGIAE TTFV
	dog	AFA SPPSGIAE TTFV
	rat	GFA SPPTDIAQ TTYV
	mouse	GFA SPPSDIEE TTYV
	chicken	AFA SPSTGIAQ TTFV
	frog	GFA SPSSGIAD ATFI
Duox	Drosophila	SFM AEHTDLRH IMGV
	zebrafish	YGL QAHSSGIP ETSM
	sea urchins	SVE REFAGLPR IAGF
	C. elegans	RYM AENRDLRR VMGA

FIGURE 11. **Alignment of the A-loops of Duox in many species.** Chicken, *Drosophila*, zebrafish, sea urchins, and *Caenorhabditis elegans* each have only one Duox. *Blue letters* in Duox1 and Duox and *red letters* in Duox2 indicate highly conserved residues between species.

Duox-DuoxA complex. Although the A-loop of Duox1 is more effective at preventing O_2^- leakage than that of Duox2, the A-loops of both the Duox isozymes function in preventing O_2^- release (Fig. 8). A recent study (33) showed that Nox4 has a unique extracellular E-loop, longer than that in other Nox family proteins, which was proposed to hinder O_2^- release and facilitate its conversion to H_2O_2. Interestingly, this study highlighted the importance of His[222] of Nox4, proposing that this conserved residue serves as a source of protons for O_2^- dismutation. However, we found that neither the E-loop nor the C-loop aa sequences of either Duox influenced O_2^- release by Duox-DuoxA complexes. The PoxH domain of Duoxes is a candidate for intramolecular O_2^- dismutation, although the isolated domains of both Duox isozymes did not demonstrate superoxide dismutase or peroxidase activity *in vitro* (24, 25). In this study we observed reduced O_2^- release by Duox(1PoxH-2)-DuoxA1 than by Duox2-DuoxA1 (Fig. 4), suggesting that the PoxH domain of Duox1 could reduce O_2^- leakage by supporting its conversion to H_2O_2. Three residues in the A-loop of Duox1 (HH and G) critical for the reduction of O_2^- leakage are highly conserved in Duox1 in many species (Fig. 11), and the corresponding PP residues in the A-loop of Duox2 are also well conserved in many species. The A-loop sequences of human Duox1 and Duox2 have different predicted secondary structures as analyzed by several structural modeling algorithms (cfPred: Chou-Fasman Protein Secondary Structure Predictor), suggesting that the A-loops of Duox1 and Duox2 interact differently with other structures involved in the conversion of O_2^- to H_2O_2 (*i.e.* the DuoxA N termini or Duox PoxH domains). These structural differences may explain the observed differences in O_2^- leakage, complex stability, and maturation. The A-loops of Nox1 and Nox5, which produce O_2^-, also lack HH residues and are even more divergent, consistent with their effects in inducing or enhancing O_2^- release by chimeric Duox1 or Duox2 proteins, respectively (Fig. 8). Moreover, the compound heterozygous mutation of Duox2(L1067S) in the A-loop combined with other Duox2 mutations was identified in patients with transient congenital hypothyroidism (12), further supporting the importance of the A-loop structure to Duox function.

We found direct binding of the A-loops of Duoxes to the N termini of DuoxAs *in vitro* (Fig. 9). In addition, the strength of the interaction between the Duox and DuoxA pairs at the cellular level inversely correlated with the amount of O_2^- released-weaker interactions correlated with greater O_2^- leakage (Fig. 10, *A* and *B*). Furthermore, the A-loop of Duox1 induced complete Endo H-resistant glycosyl modifications of Duoxes (Fig. 10*C*). To determine whether glycosyl modifications of Duoxes affect ROS production and O_2^- leakage, we created glycosylation-defective mutants of untagged and HA-tagged human Duox1 and Duox2 in which all five putative glycosylation sites (4) (Asn-94, -342, -354, -461, and -534 in Duox1; Asn-100, -348, -382, -455, and -537 in Duox2) were replaced by Gln. In Duox-reconstituted HEK293 cell systems, these mutants showed severely impaired glycosylation (almost no band shift in Duoxes upon immunoblotting), plasma membrane targeting/localization of the Duox-DuoxA complex, and ROS production or O_2^- leakage detected by luminol + HRP or Diogenes (data not shown). Taken together, these results suggest that 1) binding of the A-loop of Duox1 to the N terminus of DuoxA1 contributes to the enhanced interaction between Duox1 and DuoxA1 observed at the cellular level, thereby inducing more stable, mature Duox-DuoxA complexes than those involving Duox2, and 2) glycosyl modifications of Duoxes are essential for the targeting/localization of the Duox-DuoxA complex to the plasma membrane, increasing the stability of the Duox-DuoxA complex and developing capabilities for ROS production (including O_2^- leakage) on the plasma membrane. The formation of more stable Duox-DuoxA heterodimers or structural changes associated with maturation, which are probably acquired at the final destination, the apical cell surface, may create an environment that more efficiently supports ROS conversion and prevents O_2^- leakage.

In conclusion, in this study we demonstrated that the A-loop of Duoxes is an important structural determinant that interacts with the N termini of DuoxAs and facilitates the conversion of O_2^- to H_2O_2, likely through mechanisms promoting the stabilization and maturation of Duox-DuoxA complexes. Further studies are required to unveil the detailed mechanisms underlying the intramolecular conversion of O_2^- to H_2O_2 by the Duox-DuoxA complex.

REFERENCES

1. Quinn, M. T., Ammons, M. C., and Deleo, F. R. (2006) The expanding role of NADPH oxidases in health and disease: no longer just agents of death and destruction. *Clin. Sci.* **111,** 1–20
2. Leto, T. L., Morand, S., Hurt, D., and Ueyama, T. (2009) Targeting and regulation of reactive oxygen species generation by Nox family NADPH oxidases. *Antioxid. Redox. Signal* **11,** 2607–2619
3. Matsushima, S., Tsutsui, H., and Sadoshima, J. (2014) Physiological and pathological functions of NADPH oxidases during myocardial ischemia-reperfusion. *Trends Cardiovasc. Med.* **24,** 202–205
4. De Deken, X., Wang, D., Many, M. C., Costagliola, S., Libert, F., Vassart, G., Dumont, J. E., and Miot, F. (2000) Cloning of two human thyroid cDNAs encoding new members of the NADPH oxidase family. *J. Biol. Chem.* **275,** 23227–23233

5. Dupuy, C., Ohayon, R., Valent, A., Noël-Hudson, M. S., Dème, D., and Virion, A. (1999) Purification of a novel flavoprotein involved in the thyroid NADPH oxidase. Cloning of the porcine and human cdnas. *J. Biol. Chem.* **274,** 37265–37269
6. Grasberger, H., and Refetoff, S. (2006) Identification of the maturation factor for dual oxidase. Evolution of an eukaryotic operon equivalent. *J. Biol. Chem.* **281,** 18269–18272
7. Morand, S., Ueyama, T., Tsujibe, S., Saito, N., Korzeniowska, A., and Leto, T. L. (2009) Duox maturation factors form cell surface complexes with Duox affecting the specificity of reactive oxygen species generation. *FASEB J.* **23,** 1205–1218
8. Moreno, J. C., Pauws, E., van Kampen, A. H., Jedlicková, M., de Vijlder, J. J., and Ris-Stalpers, C. (2001) Cloning of tissue-specific genes using serial analysis of gene expression and a novel computational substraction approach. *Genomics* **75,** 70–76
9. Johnson, K. R., Marden, C. C., Ward-Bailey, P., Gagnon, L. H., Bronson, R. T., and Donahue, L. R. (2007) Congenital hypothyroidism, dwarfism, and hearing impairment caused by a missense mutation in the mouse dual oxidase 2 gene, Duox2. *Mol. Endocrinol.* **21,** 1593–1602
10. Grasberger, H., De Deken, X., Mayo, O. B., Raad, H., Weiss, M., Liao, X. H., and Refetoff, S. (2012) Mice deficient in dual oxidase maturation factors are severely hypothyroid. *Mol. Endocrinol.* **26,** 481–492
11. Donkó, A., Ruisanchez, E., Orient, A., Enyedi, B., Kapui, R., Péterfi, Z., de Deken, X., Benyó, Z., and Geiszt, M. (2010) Urothelial cells produce hydrogen peroxide through the activation of Duox1. *Free Radic. Biol. Med.* **49,** 2040–2048
12. Maruo, Y., Takahashi, H., Soeda, I., Nishikura, N., Matsui, K., Ota, Y., Mimura, Y., Mori, A., Sato, H., and Takeuchi, Y. (2008) Transient congenital hypothyroidism caused by biallelic mutations of the dual oxidase 2 gene in Japanese patients detected by a neonatal screening program. *J. Clin. Endocrinol. Metab.* **93,** 4261–4267
13. Hulur, I., Hermanns, P., Nestoris, C., Heger, S., Refetoff, S., Pohlenz, J., and Grasberger, H. (2011) A single copy of the recently identified dual oxidase maturation factor (DUOXA) 1 gene produces only mild transient hypothyroidism in a patient with a novel biallelic DUOXA2 mutation and monoallelic DUOXA1 deletion. *J. Clin. Endocrinol. Metab.* **96,** E841–E845
14. Geiszt, M., Witta, J., Baffi, J., Lekstrom, K., and Leto, T. L. (2003) Dual oxidases represent novel hydrogen peroxide sources supporting mucosal surface host defense. *FASEB J.* **17,** 1502–1504
15. El Hassani, R. A., Benfares, N., Caillou, B., Talbot, M., Sabourin, J. C., Belotte, V., Morand, S., Gnidehou, S., Agnandji, D., Ohayon, R., Kaniewski, J., Noël-Hudson, M. S., Bidart, J. M., Schlumberger, M., Virion, A., and Dupuy, C. (2005) Dual oxidase2 is expressed all along the digestive tract. *Am. J. Physiol. Gastrointest. Liver Physiol.* **288,** G933–G942
16. van der Vliet, A. (2011) Nox enzymes in allergic airway inflammation. *Biochim. Biophys. Acta* **1810,** 1035–1044
17. Ha, E. M., Oh, C. T., Bae, Y. S., and Lee, W. J. (2005) A direct role for dual oxidase in *Drosophila* gut immunity. *Science* **310,** 847–850
18. Moskwa, P., Lorentzen, D., Excoffon, K. J., Zabner, J., McCray, P. B., Jr., Nauseef, W. M., Dupuy, C., and Bánfi, B. (2007) A novel host defense system of airways is defective in cystic fibrosis. *Am. J. Respir. Crit. Care Med.* **175,** 174–183
19. Grasberger, H., El-Zaatari, M., Dang, D. T., and Merchant, J. L. (2013) Dual oxidases control release of hydrogen peroxide by the gastric epithelium to prevent helicobacter felis infection and inflammation in mice. *Gastroenterology* **145,** 1045–1054
20. Sumimoto, H. (2008) Structure, regulation and evolution of Nox-family NADPH oxidases that produce reactive oxygen species. *FEBS J.* **275,** 3249–3277
21. Ameziane-El-Hassani, R., Morand, S., Boucher, J. L., Frapart, Y. M., Apostolou, D., Agnandji, D., Gnidehou, S., Ohayon, R., Noël-Hudson, M. S., Francon, J., Lalaoui, K., Virion, A., and Dupuy, C. (2005) Dual oxidase-2 has an intrinsic Ca^{2+}-dependent H_2O_2-generating activity. *J. Biol. Chem.* **280,** 30046–30054
22. De Deken, X., Corvilain, B., Dumont, J. E., and Miot, F. (2014) Roles of DUOX-mediated hydrogen peroxide in metabolism, host defense, and signaling. *Antioxid. Redox. Signal* **20,** 2776–2793
23. Kawahara, T., Quinn, M. T., and Lambeth, J. D. (2007) Molecular evolution of the reactive oxygen-generating NADPH oxidase (Nox/Duox) family of enzymes. *BMC Evol. Biol.* **7,** 109
24. Meitzler, J. L., and Ortiz de Montellano, P. R. (2009) Caenorhabditis elegans and human dual oxidase 1 (DUOX1) "peroxidase" domains: insights into heme binding and catalytic activity. *J. Biol. Chem.* **284,** 18634–18643
25. Meitzler, J. L., and Ortiz de Montellano, P. R. (2011) Structural stability and heme binding potential of the truncated human dual oxidase 2 (DUOX2) peroxidase domain. *Arch. Biochem. Biophys.* **512,** 197–203
26. Zamproni, I., Grasberger, H., Cortinovis, F., Vigone, M. C., Chiumello, G., Mora, S., Onigata, K., Fugazzola, L., Refetoff, S., Persani, L., and Weber, G. (2008) Biallelic inactivation of the dual oxidase maturation factor 2 (DUOXA2) gene as a novel cause of congenital hypothyroidism. *J. Clin. Endocrinol. Metab.* **93,** 605–610
27. Ueyama, T., Tatsuno, T., Kawasaki, T., Tsujibe, S., Shirai, Y., Sumimoto, H., Leto, T. L., and Saito, N. (2007) A regulated adaptor function of $p40^{phox}$: distinct $p67^{phox}$ membrane targeting by $p40^{phox}$ and by $p47^{phox}$. *Mol. Biol. Cell* **18,** 441–454
28. Nauseef, W. M. (2014) Detection of superoxide anion and hydrogen peroxide production by cellular NADPH oxidases. *Biochim. Biophys. Acta* **1840,** 757–767
29. Ueyama, T., Son, J., Kobayashi, T., Hamada, T., Nakamura, T., Sakaguchi, H., Shirafuji, T., and Saito, N. (2013) Negative charges in the flexible N-terminal domain of rho GDP-dissociation inhibitors (RhoGDIs) regulate the targeting of the RhoGDI-Rac1 complex to membranes. *J. Immunol.* **191,** 2560–2569
30. Pick, E. (2014) Cell-free NADPH oxidase activation assays: "*in vitro* veritas." *Methods Mol. Biol.* **1124,** 339–403
31. Hoste, C., Dumont, J. E., Miot, F., and De Deken, X. (2012) The type of DUOX-dependent ROS production is dictated by defined sequences in DUOXA. *Exp. Cell Res.* **318,** 2353–2364
32. Cheng, G., Cao, Z., Xu, X., van Meir, E. G., and Lambeth, J. D. (2001) Homologs of gp91phox: cloning and tissue expression of Nox3, Nox4, and Nox5. *Gene* **269,** 131–140
33. Takac, I., Schröder, K., Zhang, L., Lardy, B., Anilkumar, N., Lambeth, J. D., Shah, A. M., Morel, F., and Brandes, R. P. (2011) The E-loop is involved in hydrogen peroxide formation by the NADPH oxidase Nox4. *J. Biol. Chem.* **286,** 13304–13313